Tunnels
Underground Excavations

Design Analyses
Case Studies and Observed Performance

Giovanni Barla

Department of Structural and Geotechnical Engineering

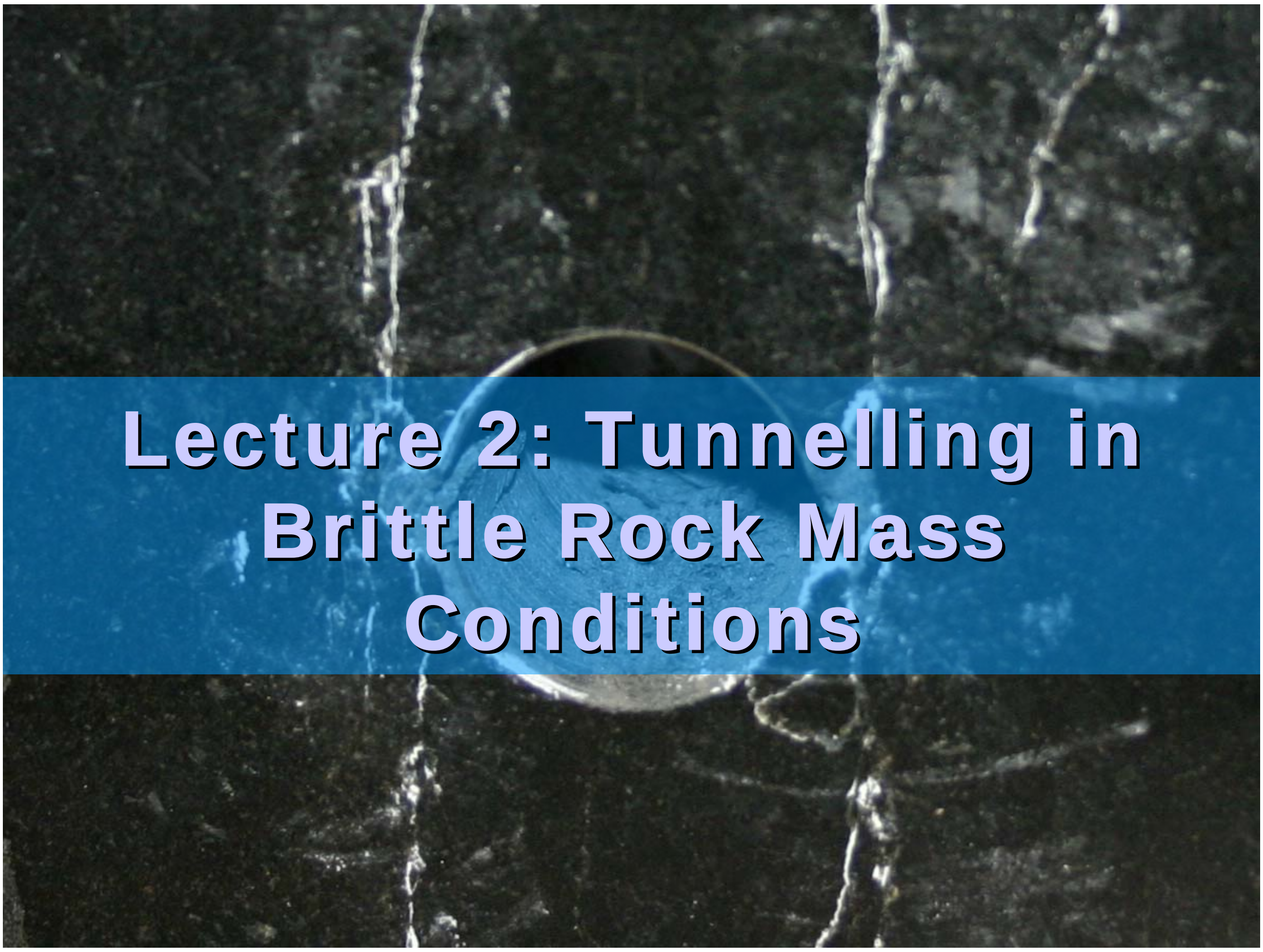

Lecture 2: Tunnelling in Brittle Rock Mass Conditions

Lecture Outline

- Introduction
- Laboratory Results
- Field Evidence
- Modelling Brittle Failure
- Case Study
- Conclusions

BRITTLE FAILURE

BRITTLE FAILURE takes place around underground openings in massive to moderately jointed rock masses subjected to high in situ stresses. It manifests itself in the form of **spalling** resulting in a revised stable geometry with the onset of V-shaped notches. The extent and depth of failure is a function of the in situ stress magnitudes relative to the rock mass strength

BRITTLE FAILURE

The onset of wall yield due to boundary compression around an underground opening is one of the primary design issues in hard rock tunnelling at depth by tunnel boring machines or conventional excavation methods. In this lecture we will discuss spalling instabilities, although in cases the interest need be centred on dynamically induced tunnel failures such as rockbursts

DUCTILE vs BRITTLE BEHAVIOUR

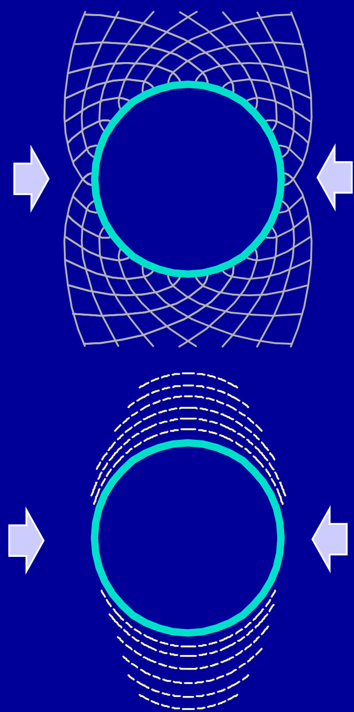

- *Yield in weak rock is controlled by continuum plastic shear slip. This is rarely observed in hard rock underground excavations*
- *Short and medium term strength in hard rock is observed to be the result of extension cracking and spalling*

Spalling Failure

Extension Crack
Propagation
under compression

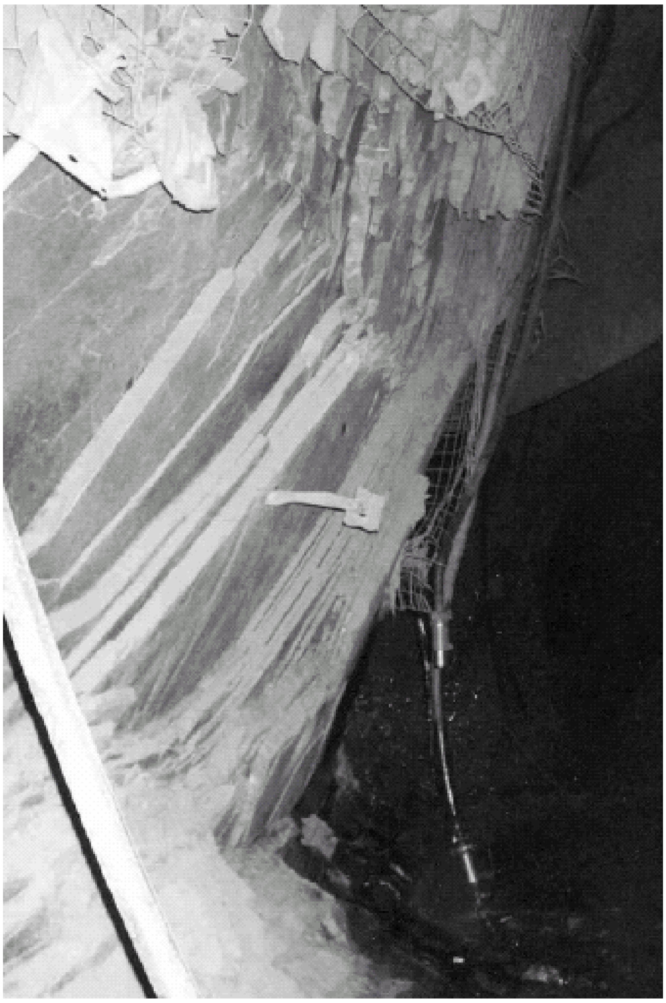

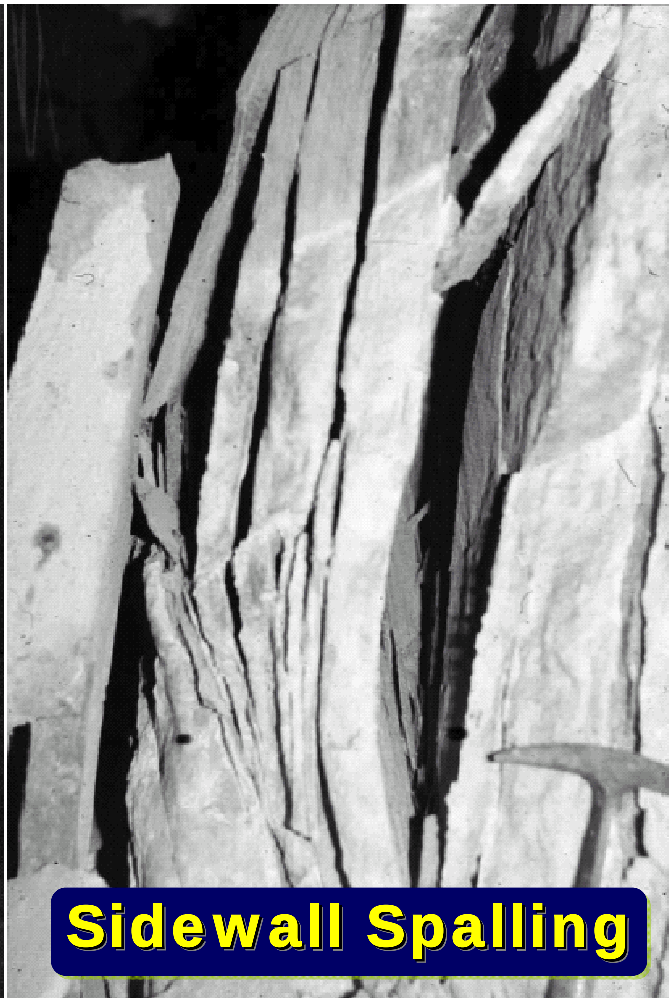

Sidewall Spalling

Rockbursts

Spalling
+
Rapid Energy Release

(Photographs: courtesy of M. Diederichs)

Rock Susceptibility to SPALLING

- Tensile damage dominates initial yield process
- Low Ratio of Compressive Strength, σ_c to Tensile Strength, σ_t

$\sigma_c / \sigma_t < 6$ = Very Low
$6 < \sigma_c / \sigma_t < 8$ = Low
$8 < \sigma_c / \sigma_t < 10$ = Medium
$10 < \sigma_c / \sigma_t > 15$ = High
$15 < \sigma_c / \sigma_t$ = Very High

Diederichs 2005

Rock Susceptibility to ROCKBURSTING

- If σ_c / σ_t is medium to very high rockburst potential for rock can be determined from σ_c (rock strength required to store energy)

$\sigma_c < 60$ MPa	= Very Low
$60 < \sigma_c < 80$	= Low
$80 < \sigma_c < 120$	= Medium
$120 < \sigma_c > 150$	= High
$150 < \sigma_c$	= Very High

Diederichs 2005

Spall/Burst Potential

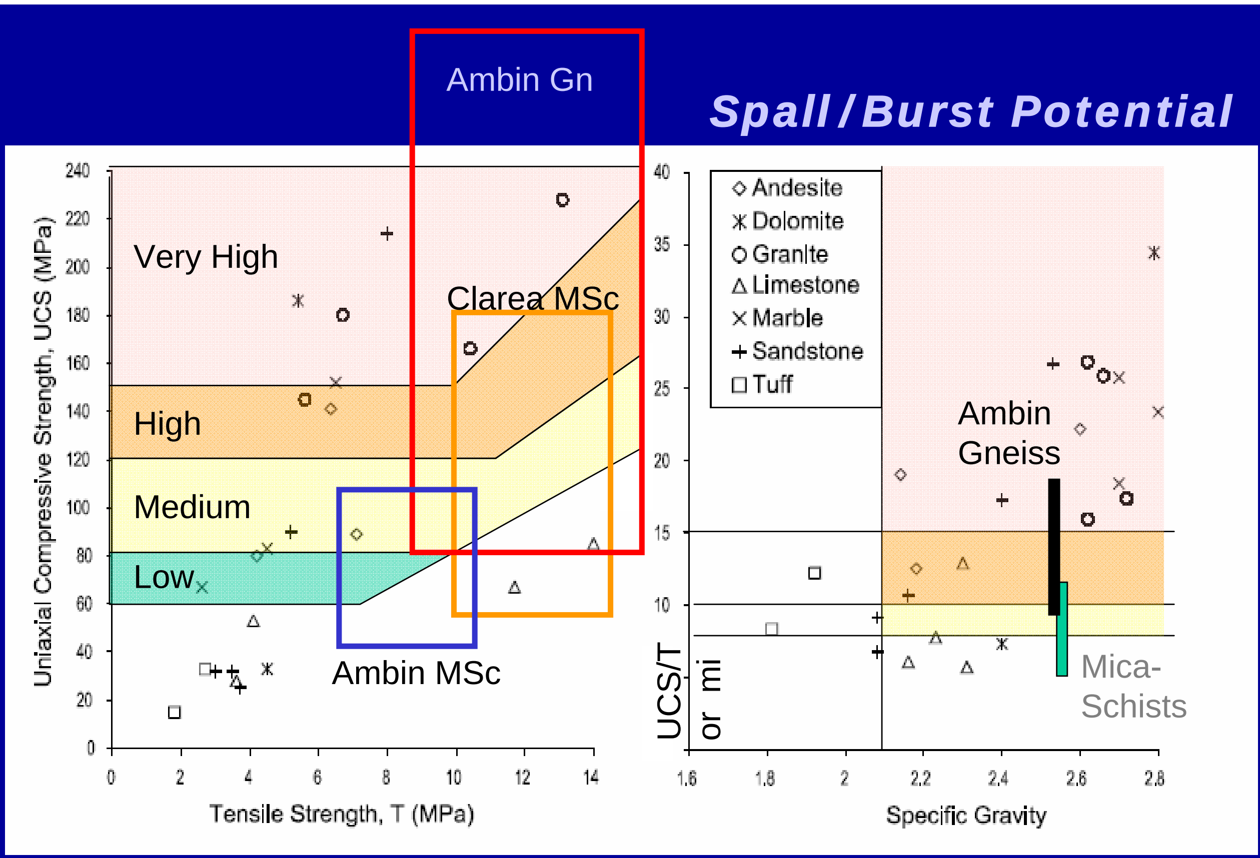

Porous rocks = No Spalling

Diederichs 2005

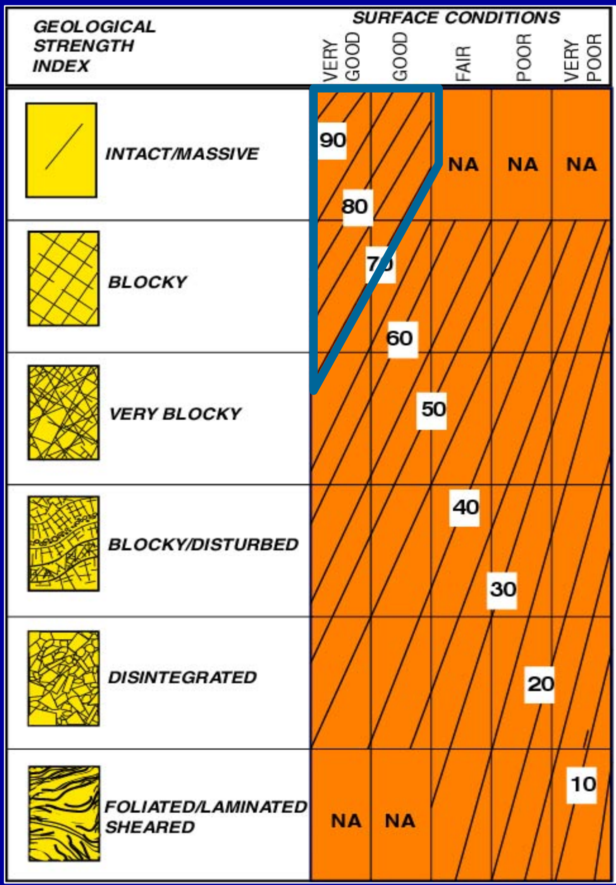

Normally Spalling (and Rockbursts) do not occur below GSI = 60

Most Likely when GSI > 70

Diederichs 2005

The starting point in the understanding of this type of behaviour is to analyse laboratory test results on cylindrical samples

It is worth to notice that a significant contribution to this understanding has been derived from recent discrete element simulations of Lac du Bonnet granite (Diederichs et al.2004)

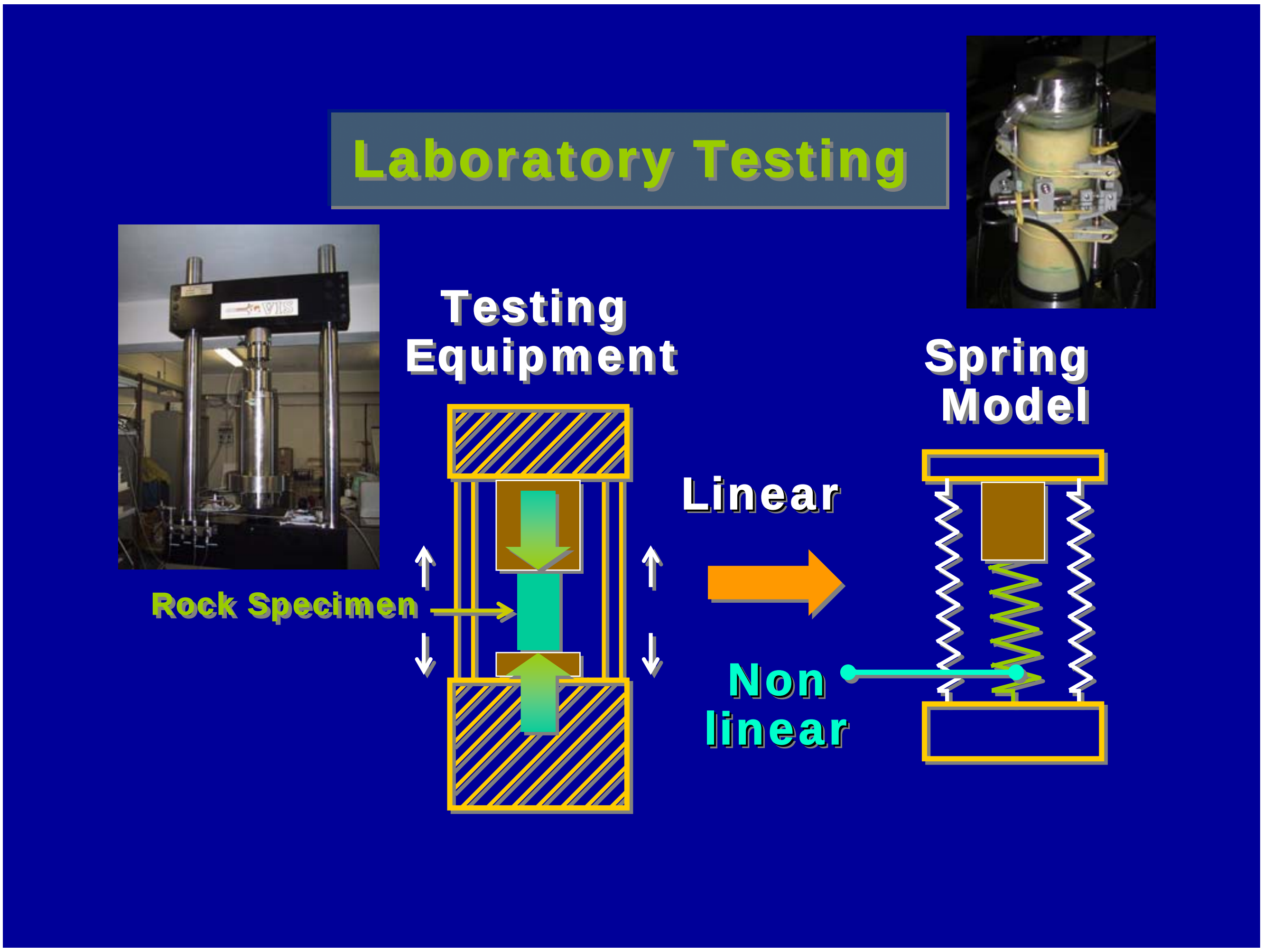

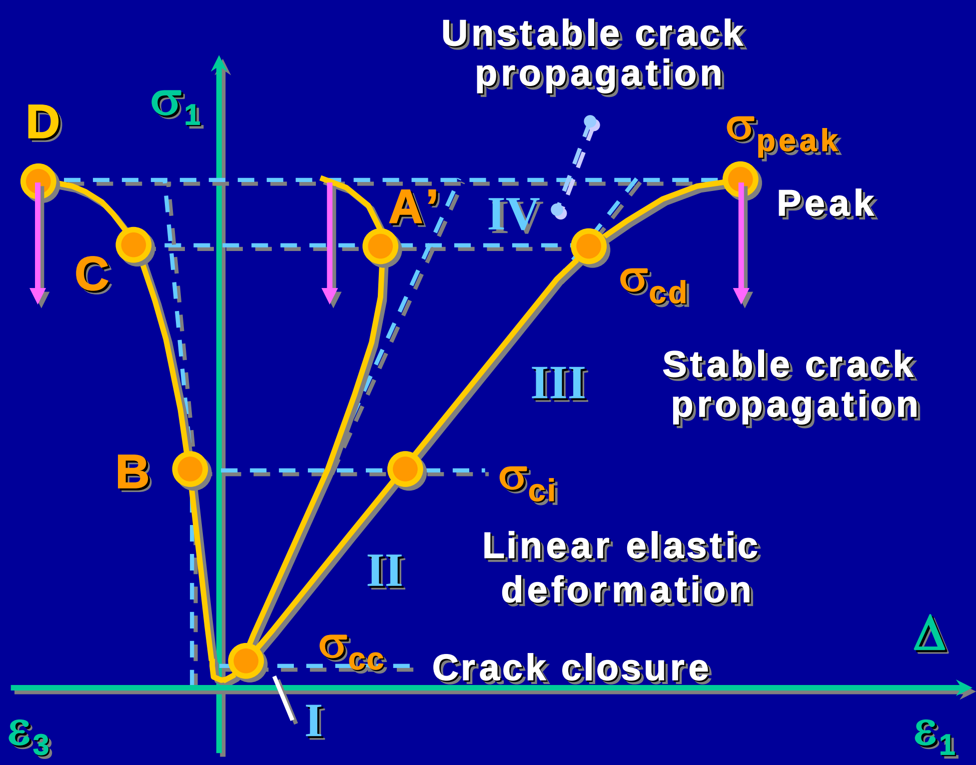

Stages of stress-strain and acoustic response in uniaxial testing (Bieniawski 1967, Eberhardt et al. 1998)

Major thresholds within a stress-strain test on rock samples coupled with acoustic emissions monitoring

- Crack closure, σ_{cc}
- Crack initiation, σ_{ci}
- Crack damage, σ_{cd}
- Peak strength, σ_{peak}

Laboratory Testing

Diederichs et al. 2004

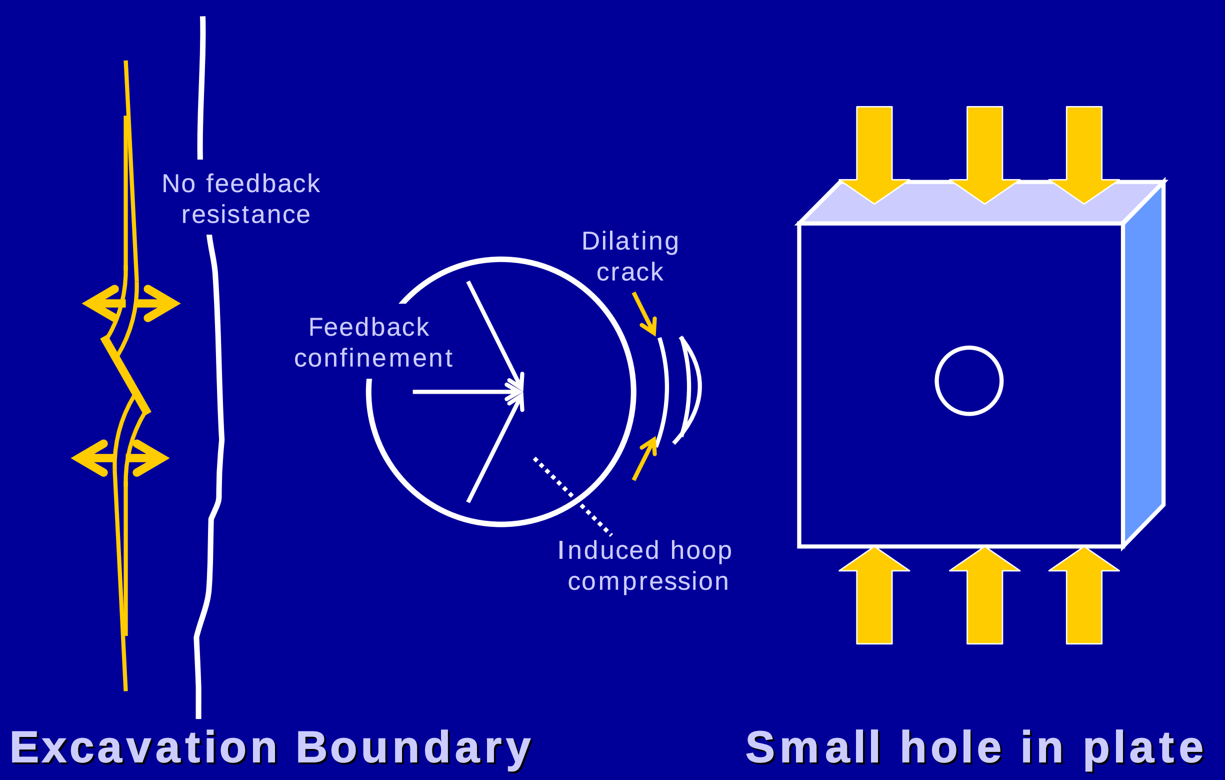


Biaxial tests run for Politecnico di Torino
at Dresden University


Biaxial tests run for Politecnico di Torino
at Dresden University

Brittle Failure
Field Observations

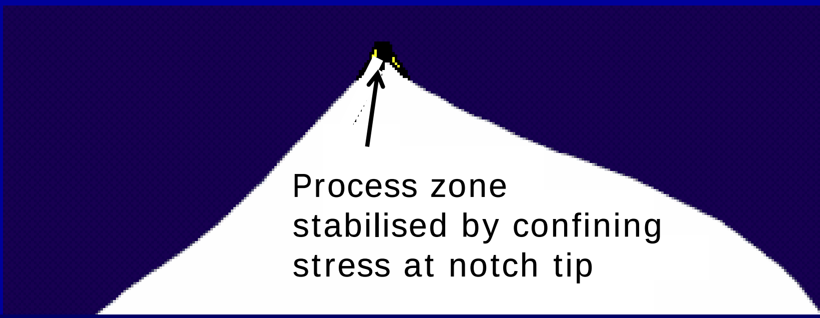

Stage IV - Stabilization: Development of the notch stops when the notch geometry provides sufficient confinement to stabilize the process zone at the notch tip. This usually means there is a slight "*tear-drop*" like curvature to the notch shape. Alternatively, if the slabs from the notch flanks are held in place by artificial support, notch development will also stop

Martin et al. 1997

The notch development is a 3D process which is directly linked to the tunnel advance

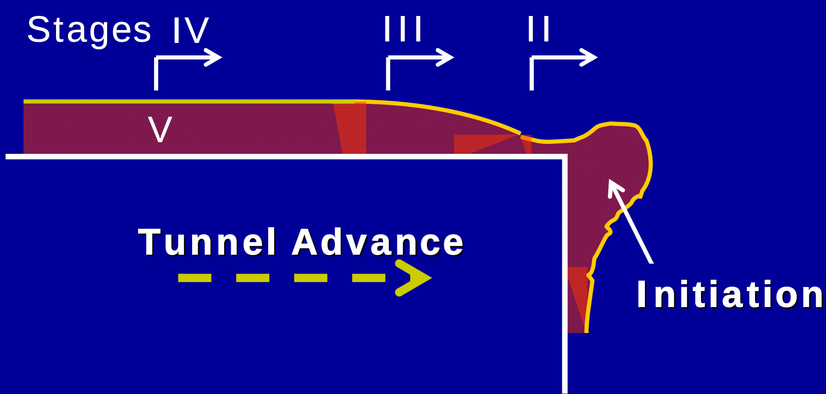

Tunnel Longitudinal Section

Martin et al. 1997

Brittle Failure
Field Observations

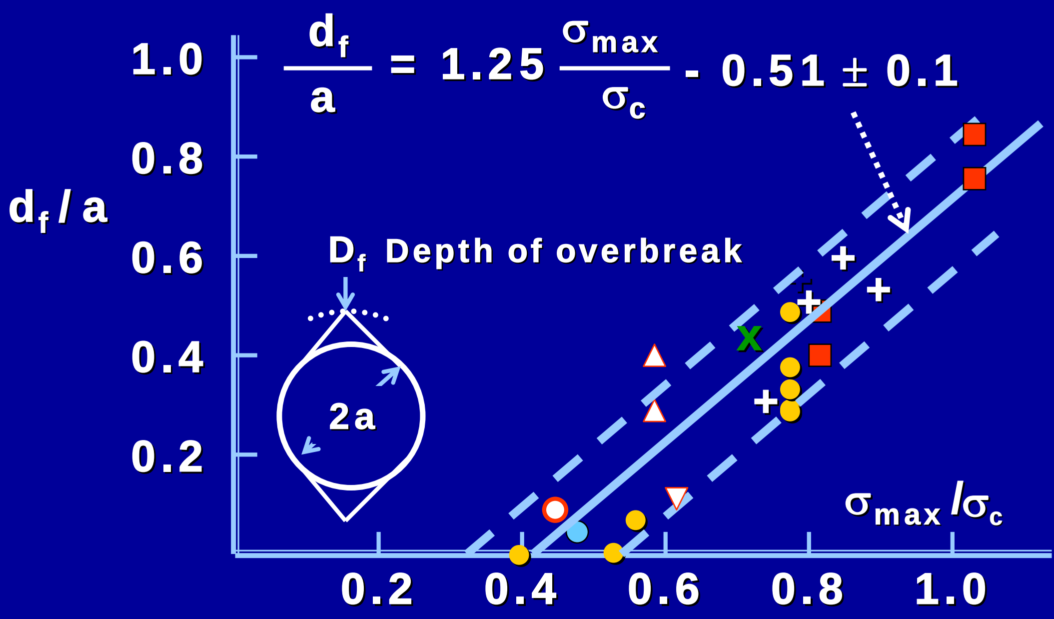

Kaiser et al. 1995

This collection of available tunnel overbreak data shows that

(1) Stress induced fracturing initiates at approximately 0.3-0.5 σ_c and the critical deviatoric stress for yield is essentially independent of confining stress

(2) No overbreak occurs at a maximum boundary stress equivalent to 40% of the compressive strength. This is a lower bound strength as unfailed tunnels are not plotted

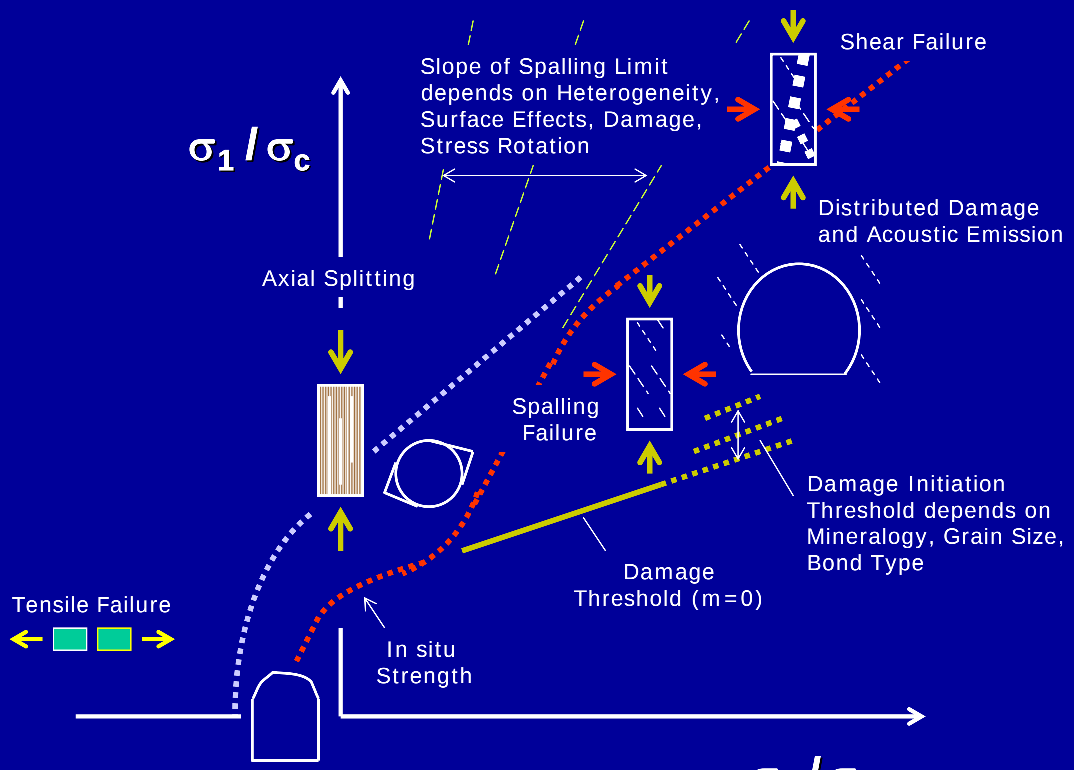

Diederichs et al. 2004

A number of possible approaches

(1) Phenomenological Models: use appropriate constitutive equations which should describe the brittle failure processes based on back analysis of carefully documented case histories

(2) Micromechanical Models: account for microscopic aspects of rock fracture and/or crack propagation mechanisms

We discuss (1) only

One common approach to estimate the yield potential and the depth of disturbance for a tunnel is the Hoek and Brown Criterion for rock mass

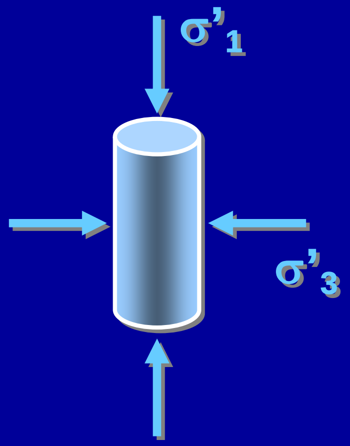

$$\sigma_1' = \sigma_3' + \sigma_c \left(m_b \frac{\sigma_3'}{\sigma_c} + s \right)^{\alpha}$$

σ_c Standard uniaxial compressive strength

s, m_b, α Costants which depend upon the characteristics of the rock mass

determined using the GSI index

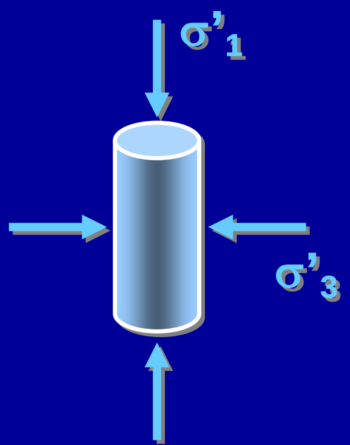

It is found that this approach is of limited reliability to predict brittle failure for rock masses of good quality, typically GSI > 70-75

m_b=0 Model

At low confinement levels, the accumulation of significant rock damage, equivalent to loss of cohesion (i.e. m_b=0), ocurs when $\sigma'_1 - \sigma'_3$ = 1/3 to 1/2 σ_c (i.e. when s= 0.11 to 0.25)

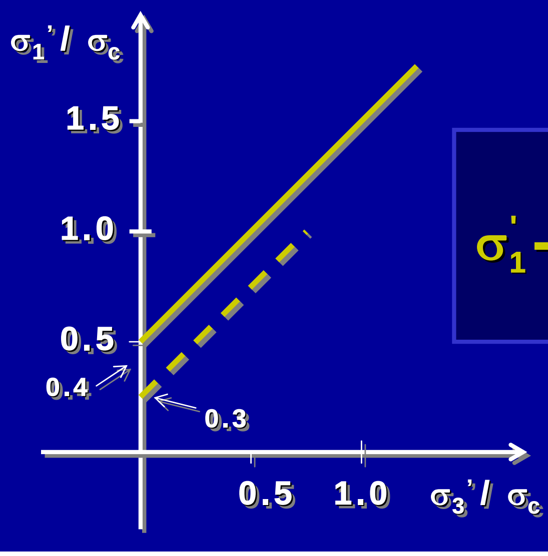

$$\sigma'_1 - \sigma'_3 = (s)^{1/2} \sigma_c = 0.33\text{-}0.50\ \sigma_c$$

Kaiser et al. 2000

CWFS Model

The **cohesive strength** is gradually destroyed by tensile cracking and crack coalescence. The **frictional strength** can be mobilized only when the cohesive strength is significantly reduced

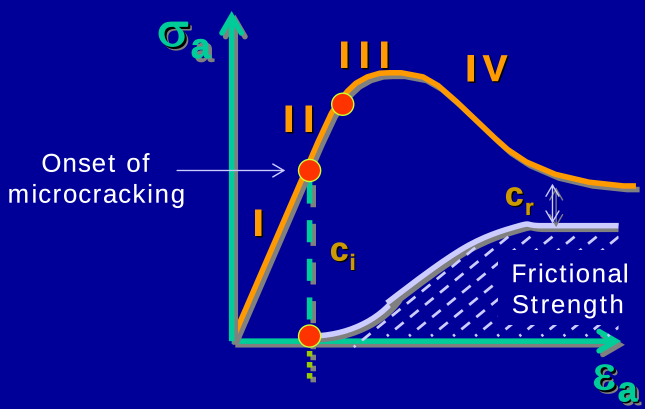

Strength components are strain- dependent

Hajiabdolmajid et al. 2002

Pont Ventoux - Susa Hydropower System

DIAMETER: 4.75 m
TOOLS: 35 cutting disks
MAXIMUM THRUST: 6950 kN
TOTAL POWER: 895 kW

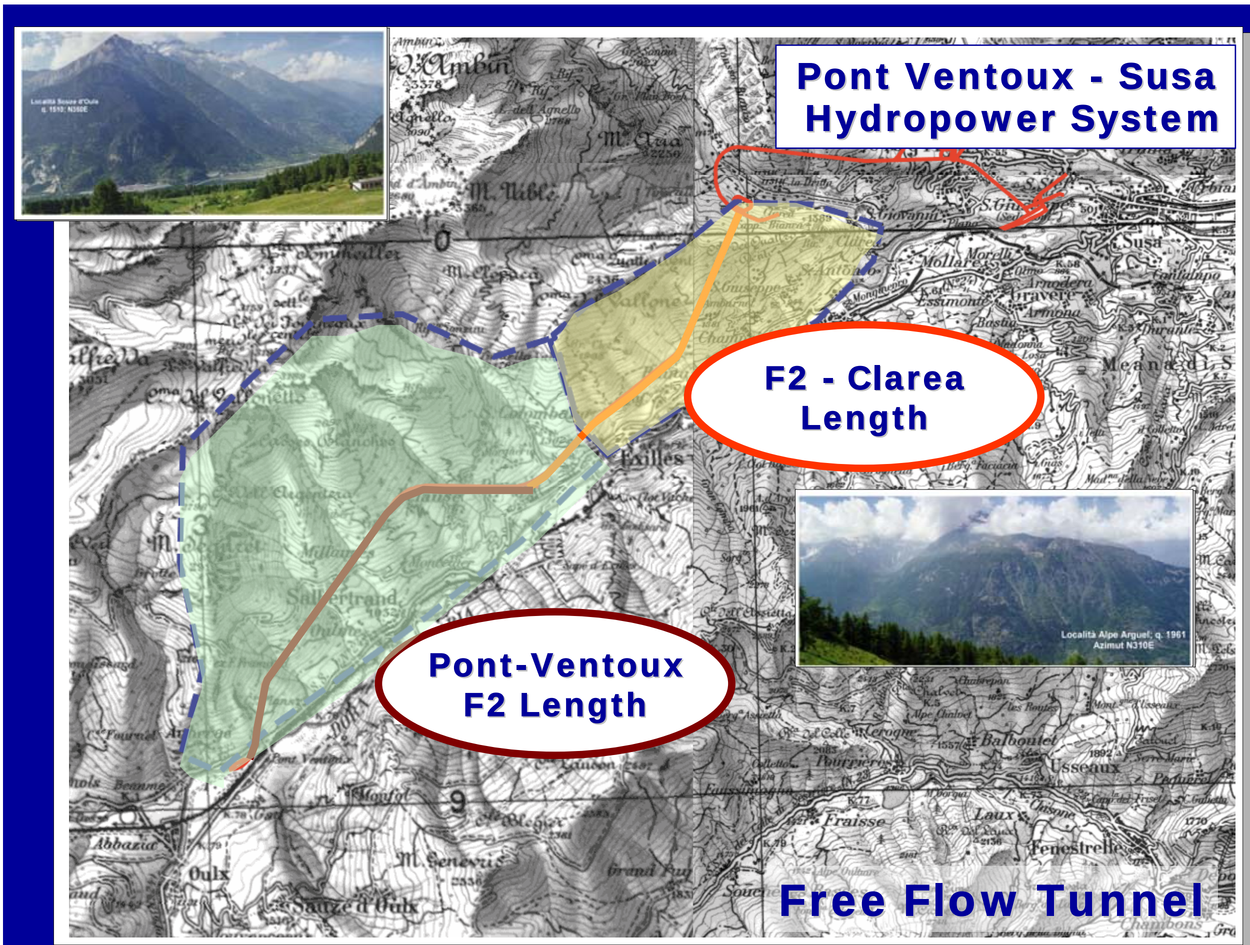

Val Clarea – F2 LENGTH

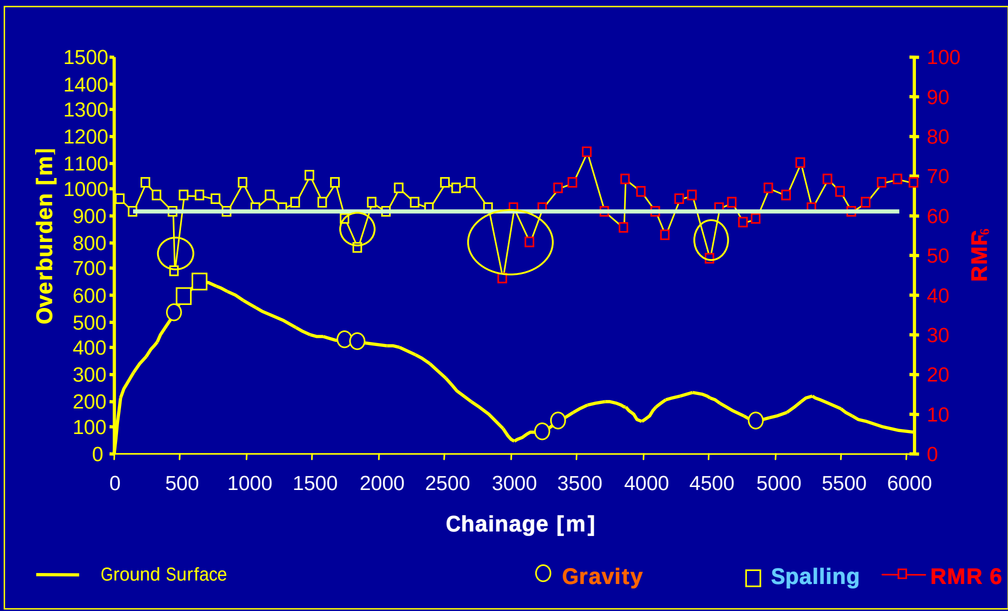

Instability of rock wedges occurs with Rock Mass Quality Index RMR < 55

Spalling instability is observed to take place when the overburden is greater than 500-600 m and RMR > 65

SECTION 1 (530-545 m)

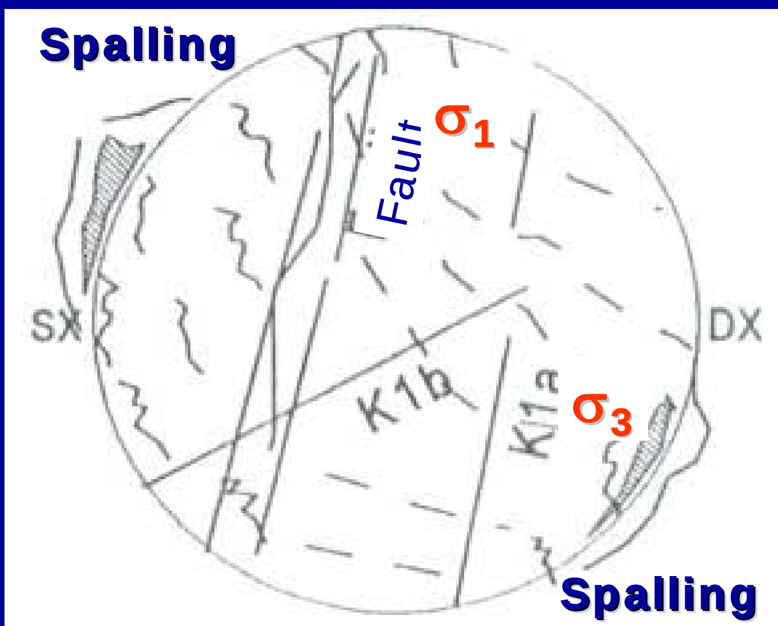

The overbreak zones give the directions of σ_1 and σ_3 . From Flat Jack measurements the Stress

Ratio is in the range 0.25 to 0.50

SECTION 2 (550-565 m)

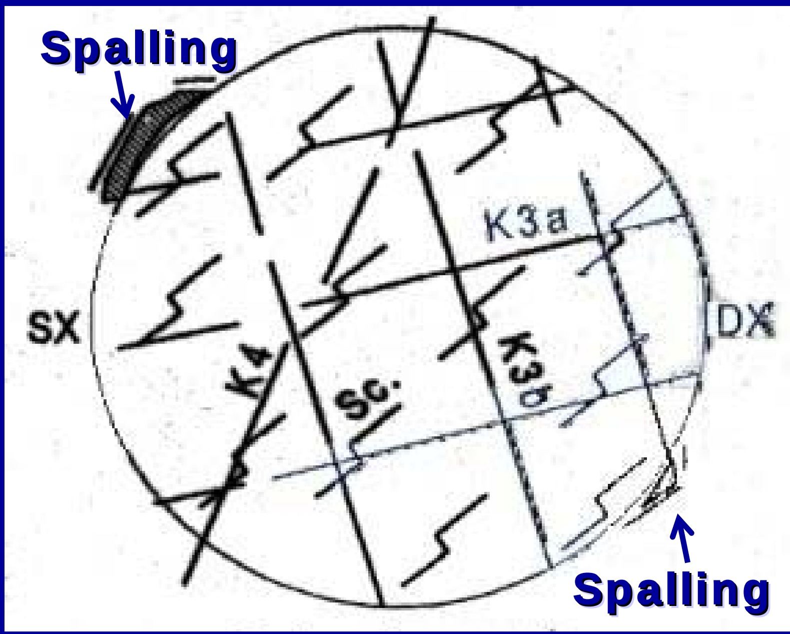

The overbreak zones give the directions of σ_1 and σ_3 . From Flat Jack measurements the Stress

Ratio is in the range 0.25 to 0.50

Intact Rock (Ambin Formation)

Gneiss

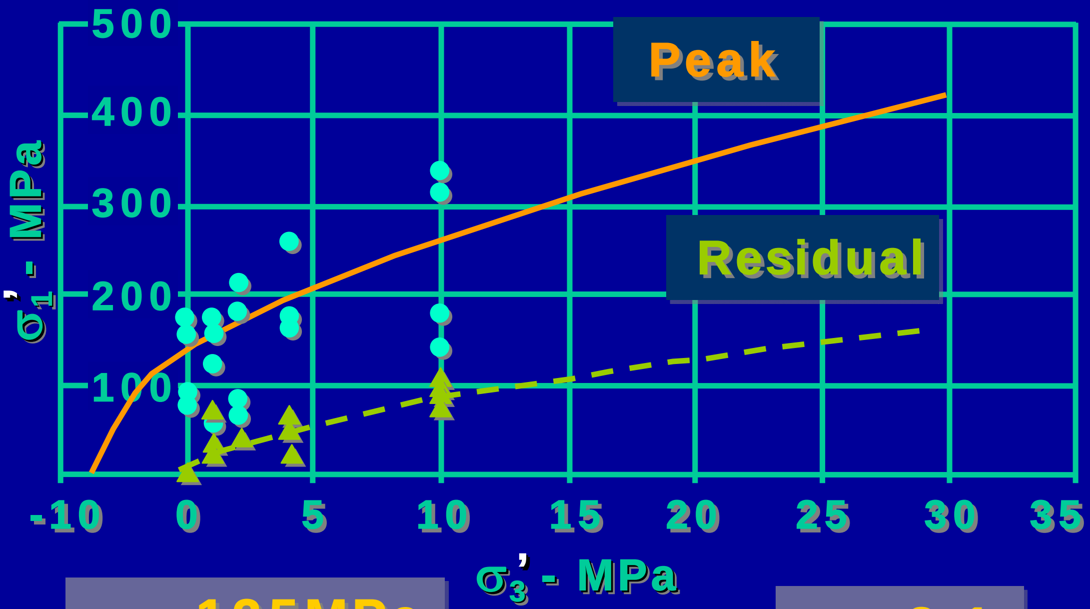

$\sigma_{ci} = 135 MPa$

$m_i = 8.1$

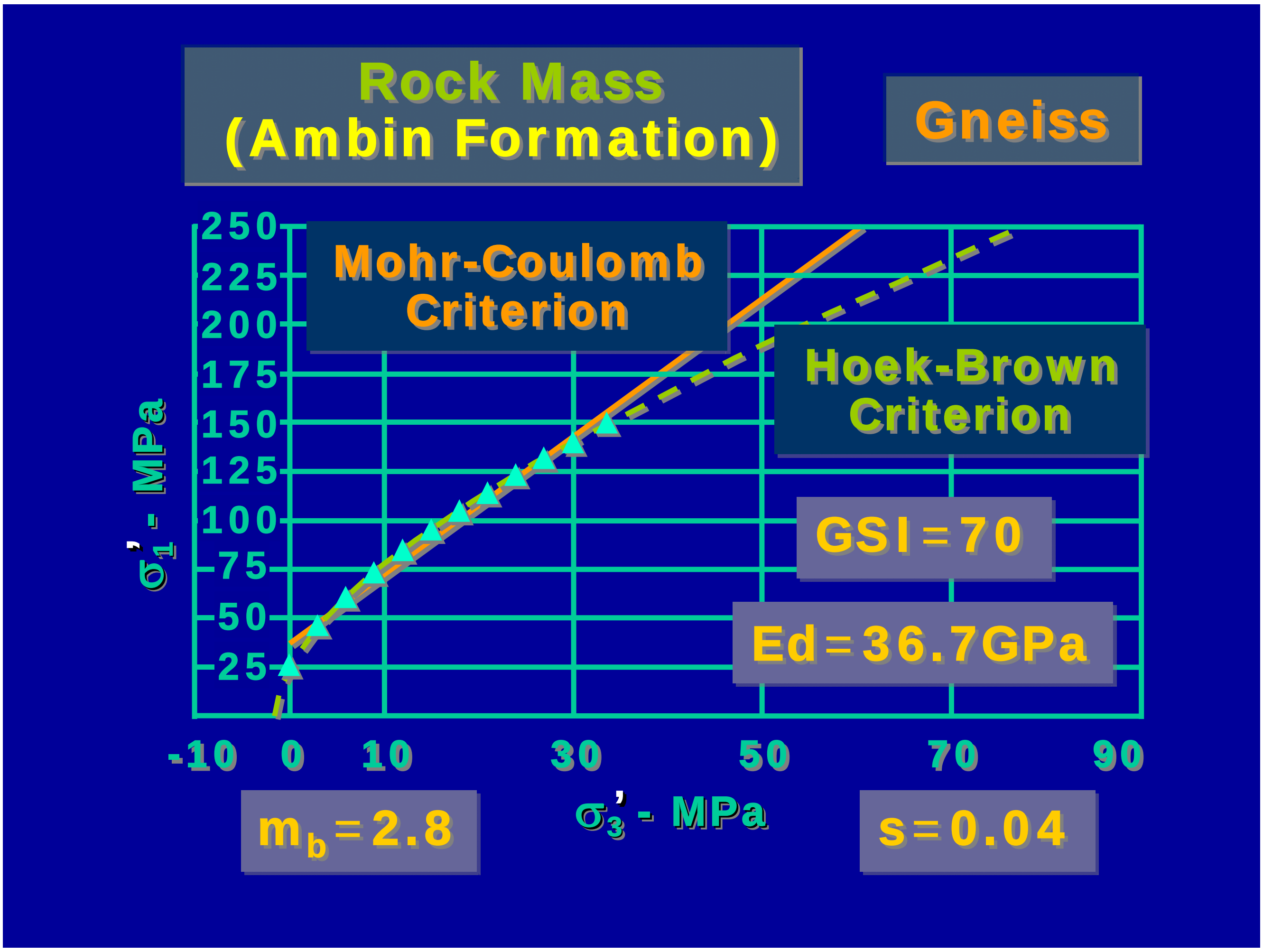

Rock Mass
(Ambin Formation)
Gneiss
Mohr-Coulomb Criterion
Hoek-Brown Criterion
GSI=70
Ed=36.7GPa
m_b=2.8
s=0.04
σ'1 - MPa
σ'3 - MPa
250
225
200
175
150
125
100
75
50
25
-10
0
10
30
50
70
90

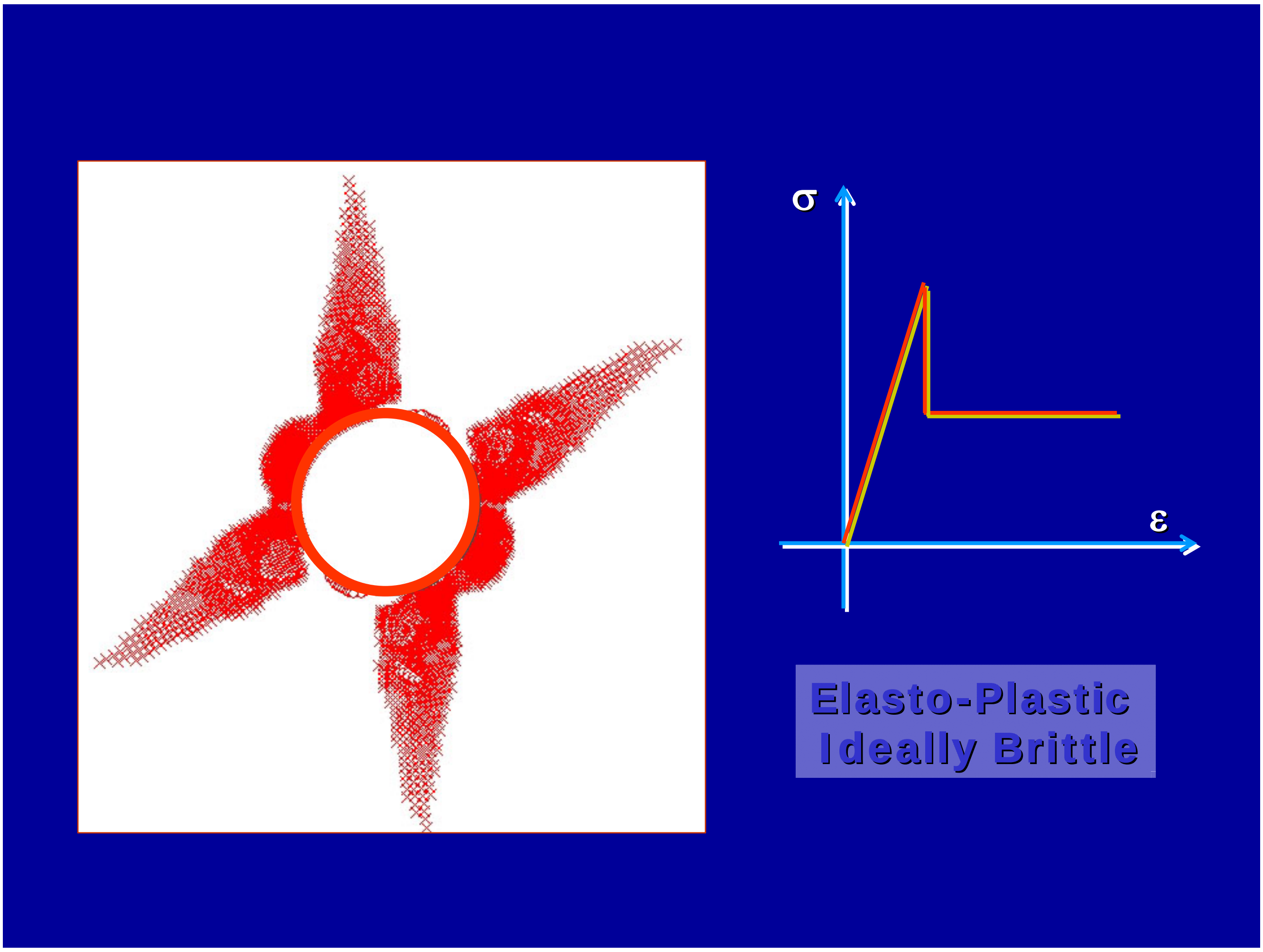

σ
ε
Elasto-Plastic
Ideally Brittle

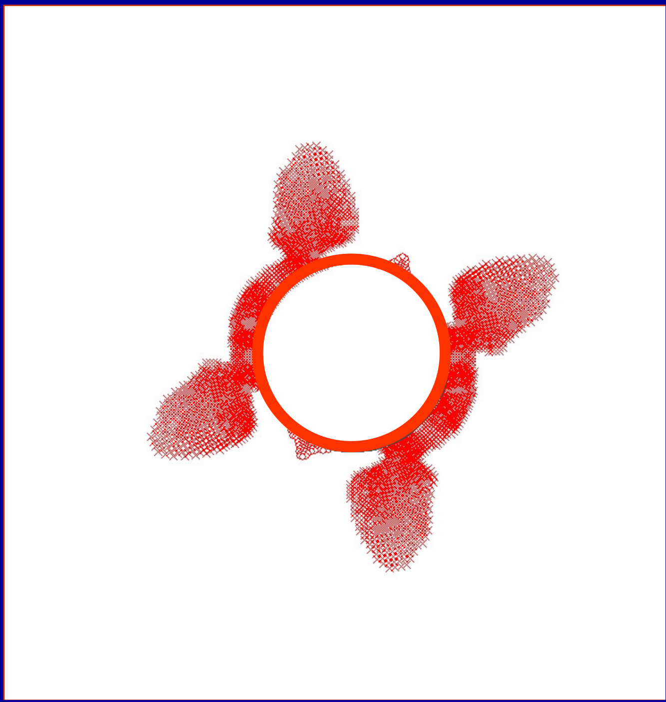

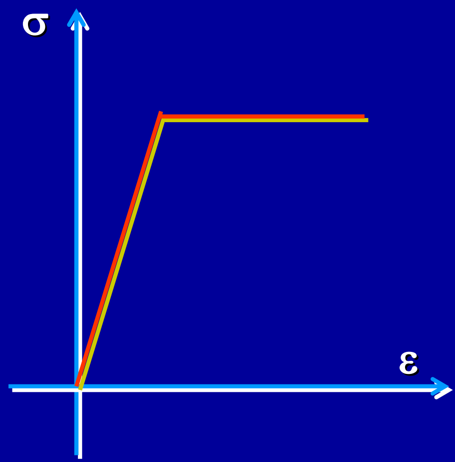

Elastic
Ideally Plastic

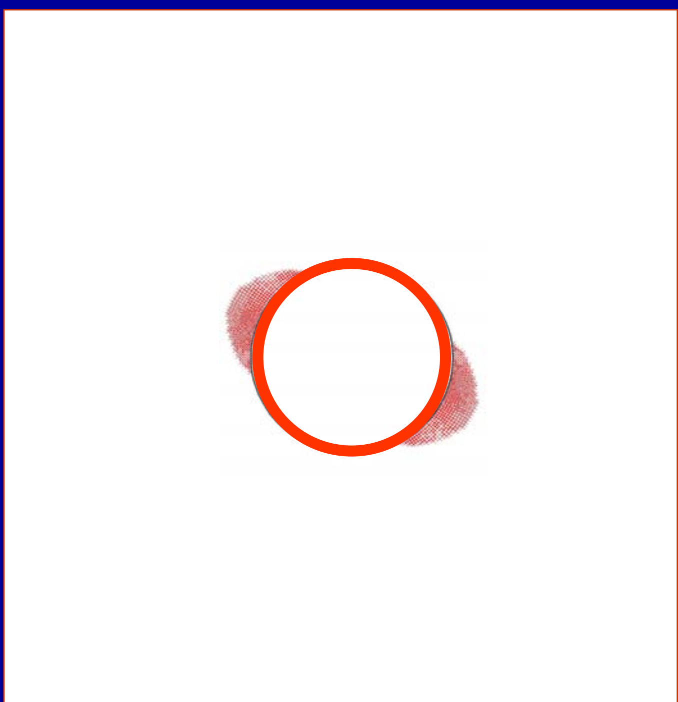

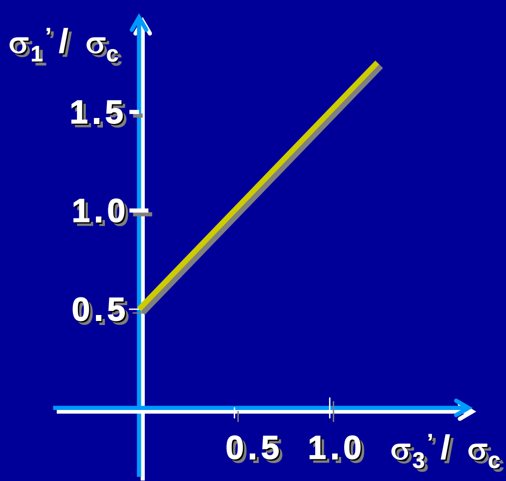

m=0 and CWFS Models
$s_b = 0.25$, $\sigma_c = 80MPa$

F2 - Val Clarea LENGTH

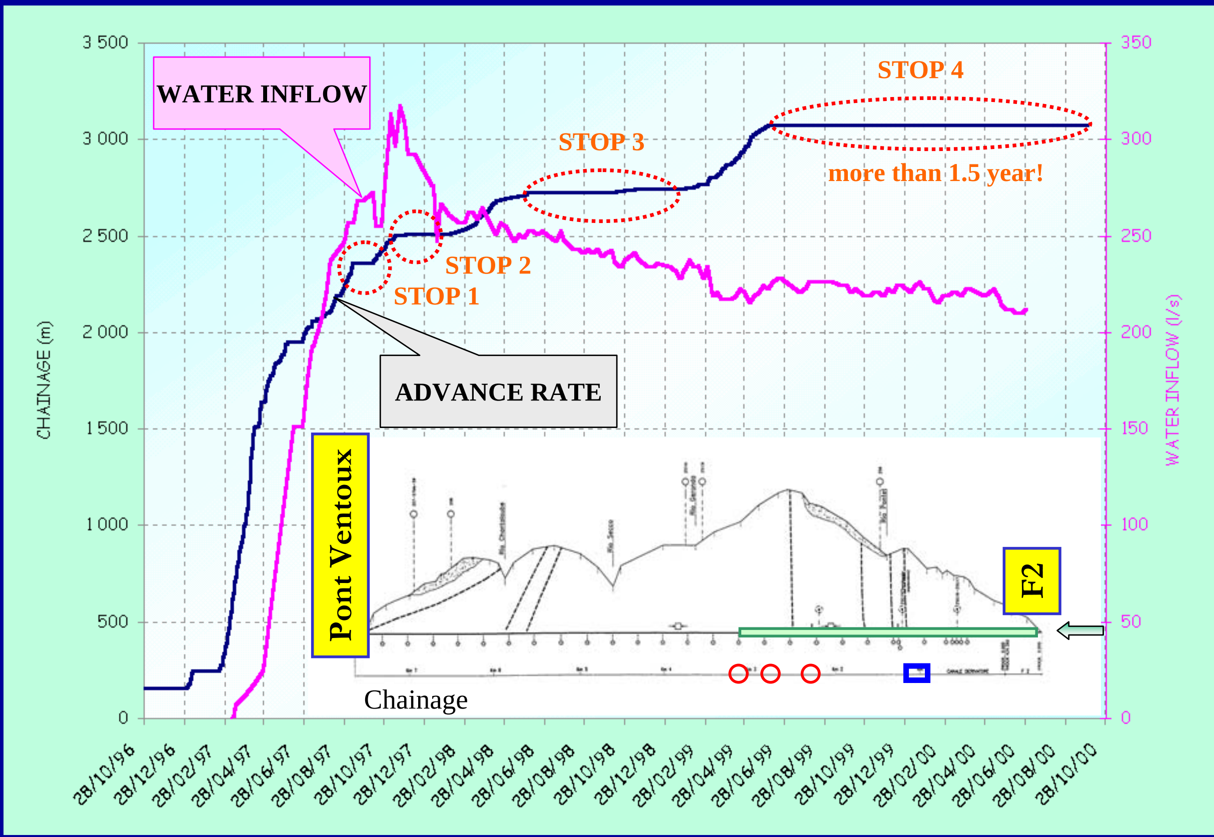

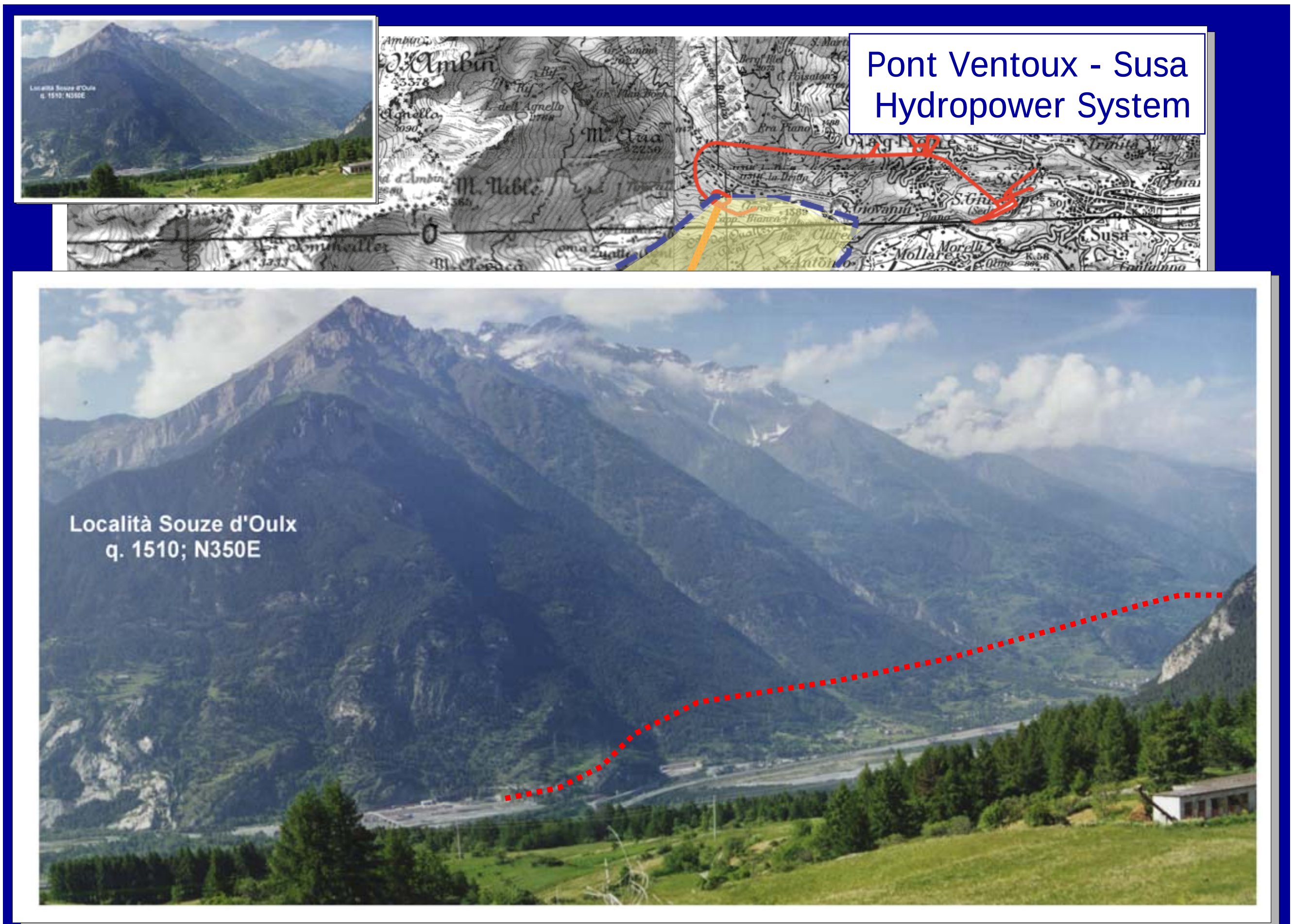

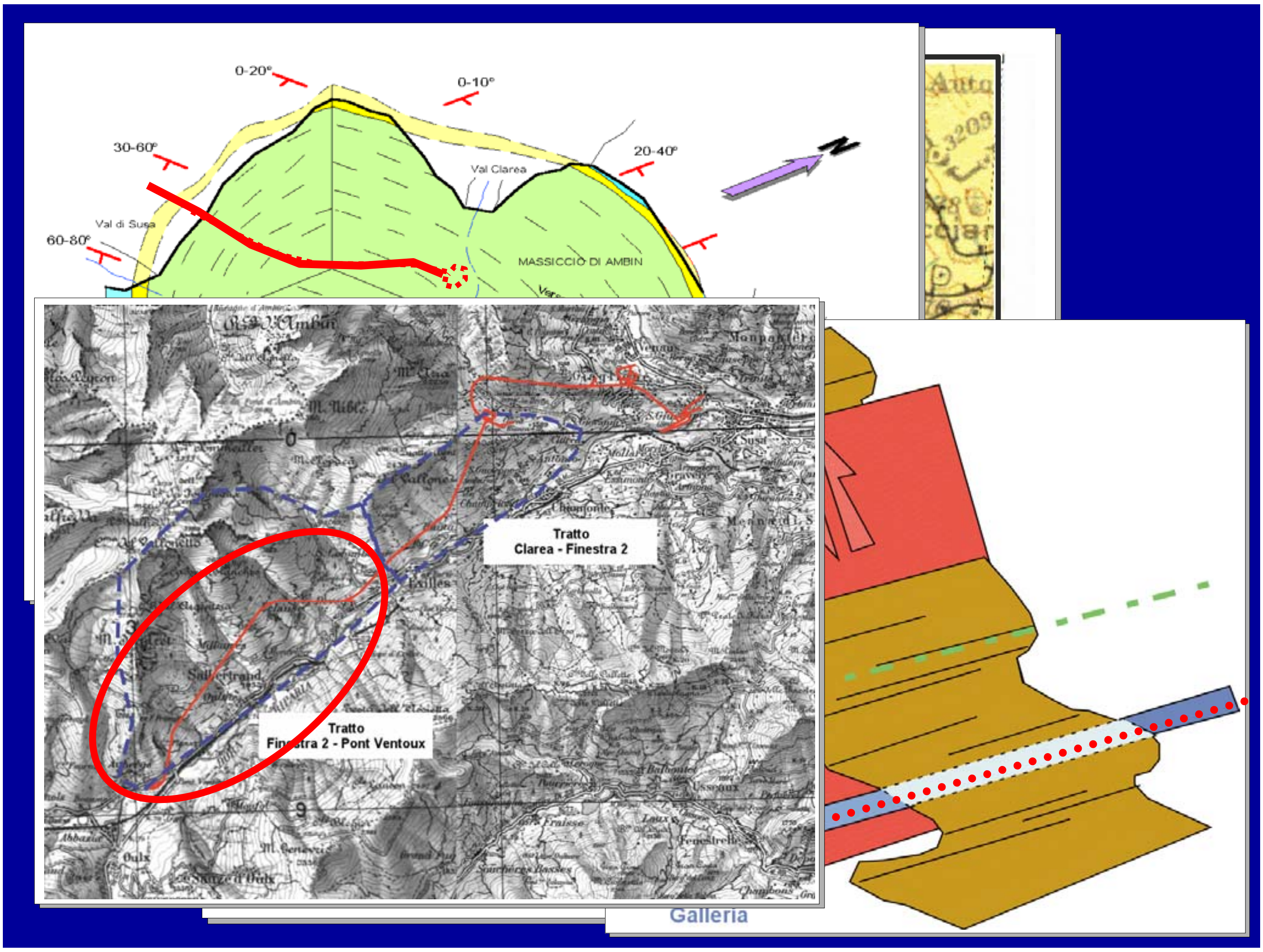

TBM's PERFORMANCE FOR THE FIRST 3070 m TUNNEL LENGTH

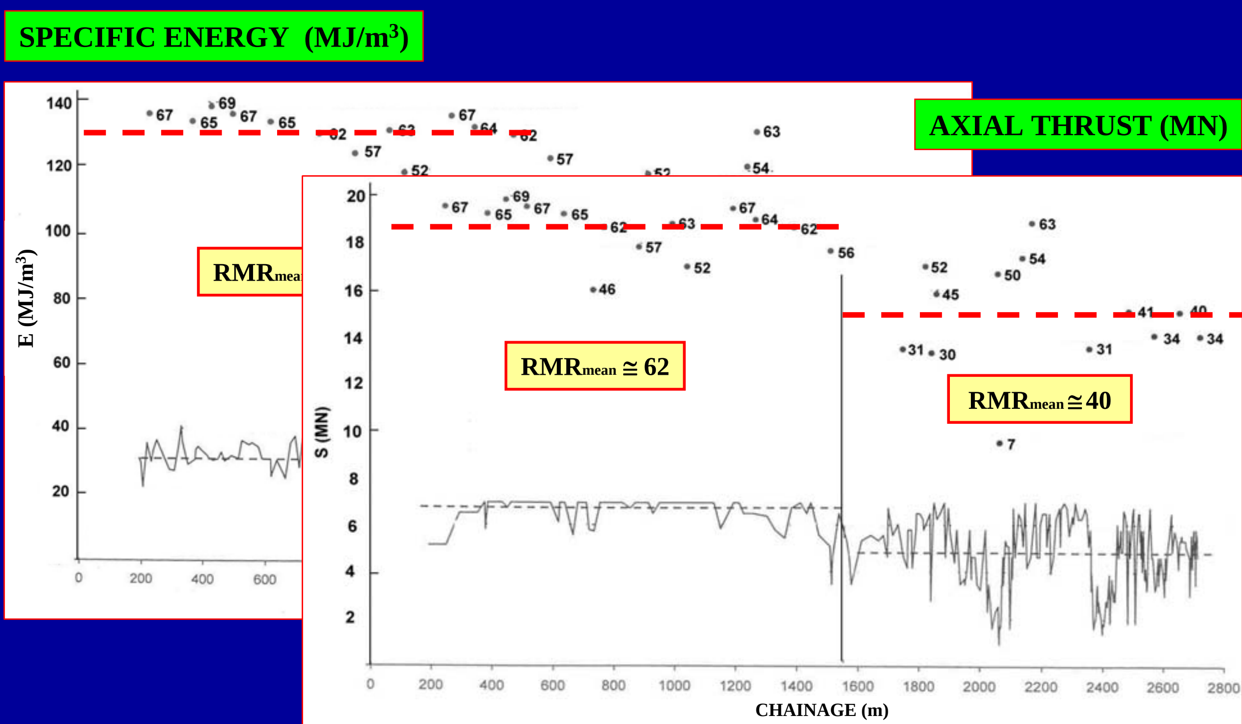

Hydroelectric System
Pont Ventoux - Susa
Chainage 0-1500 m

Hydroelectric System
Pont Ventoux - Susa

LEFT

RIGHT

PONT VENTOUX - CLAREA F2
TUNNEL
CH 2320

INTACT ROCK

Uniaxial compressive strength (peak value) $\sigma_{c,\,p}$ = 135 MPa
Uniaxial compressive strength (residual value) $\sigma_{c,\,r}$ = 10 MPa
Hoek-Brown constant (peak) $m_{i,\,p}$ = 8.1
Hoek-Brown constant (residual) $m_{i,\,r}$ = 56.1

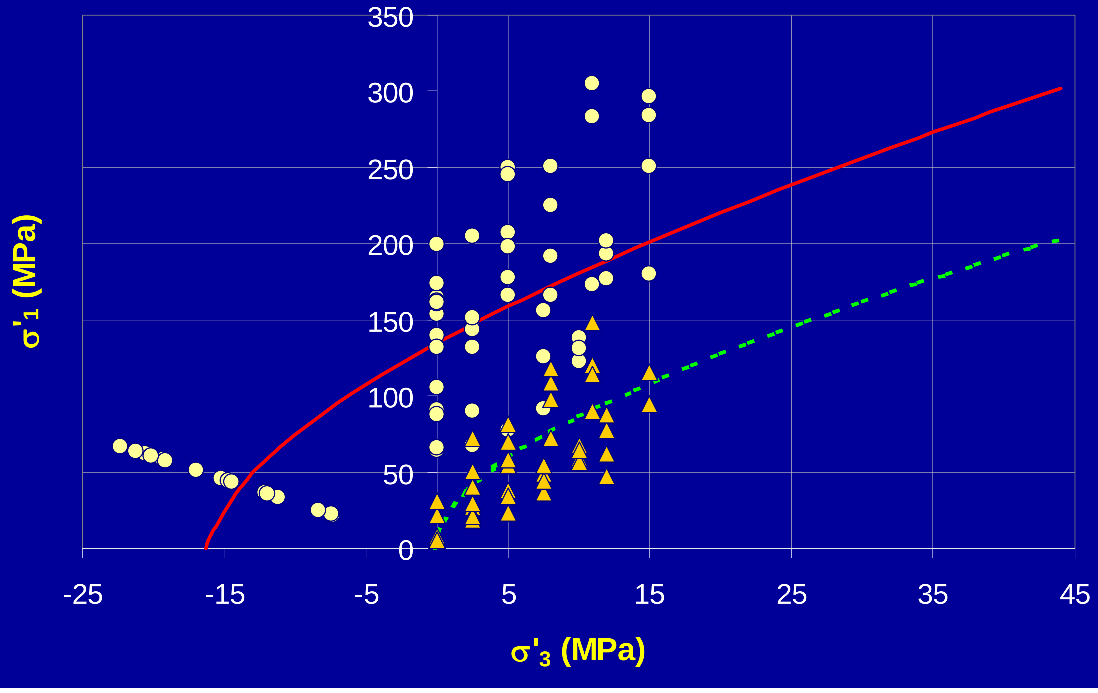

EQUIVALENT-CONTINUUM MODEL

Intact rock uniaxial compressive strength σ_{ci} = 135 MPa
Hoek-Brown constant (ir) m_i = 8.1
Geological Strength Index GSI = 70
Hoek-Brown constant (rm) m_b = 2.8
Hoek-Brown constant (rm) s = 0.04
Rock mass uniaxial compressive strength σ_{cm} = 36.7 MPa
Deformation modulus E_d = 35 GPa

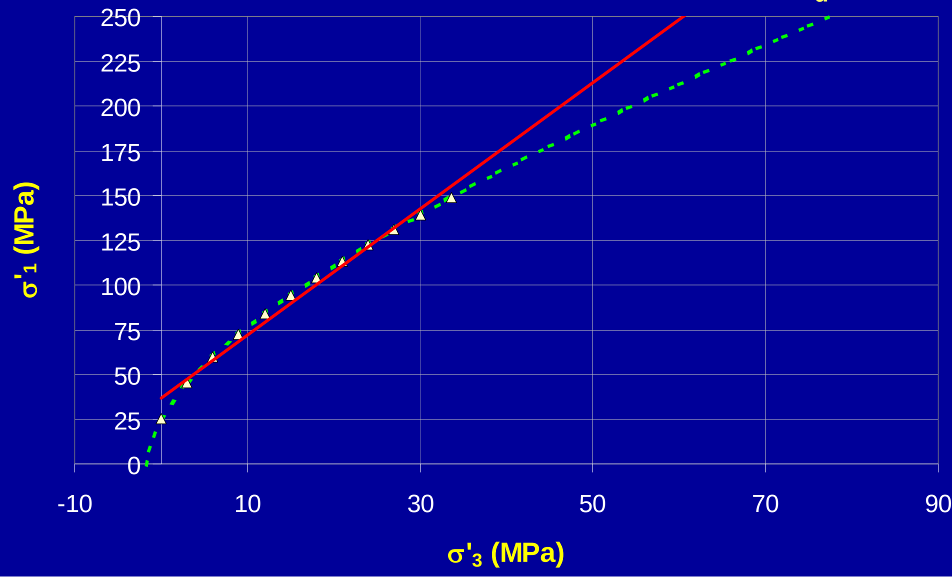

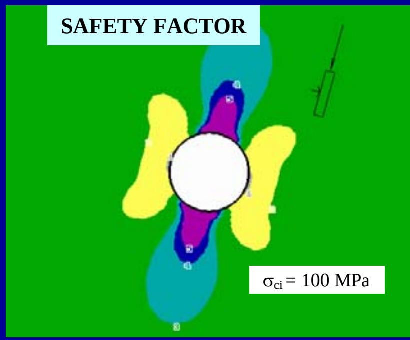

m= 0 approach, s=0.25

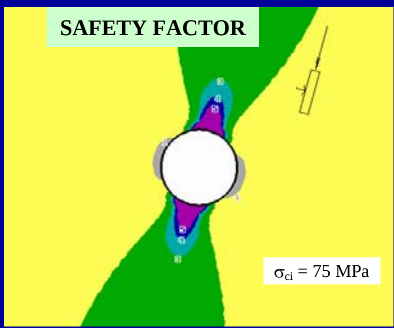

m= 0 approach, s=0.25

FAULT ZONE AT CH 2359 m

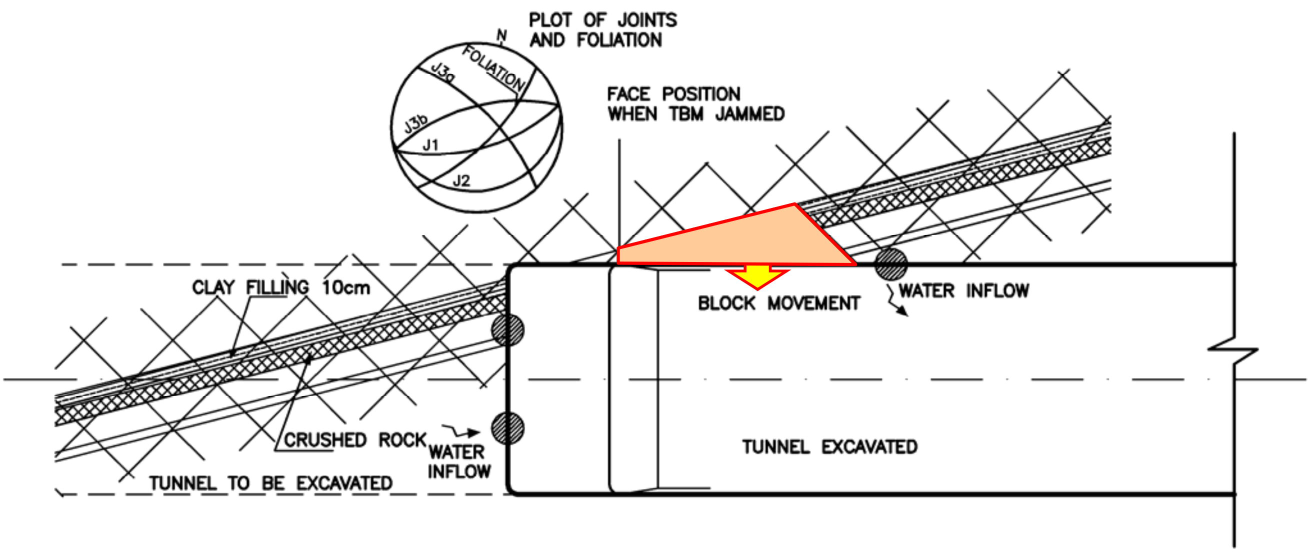

BLOCK MOVEMENT ON LEFT WALL

FAULT ZONE AT CH 2359 m

WATER FLOW AT THE TUNNEL WALL

3D Discrete Fracture Network model created by the Fracman code with plot of joint sets. This is typical of rock conditions on the right wall

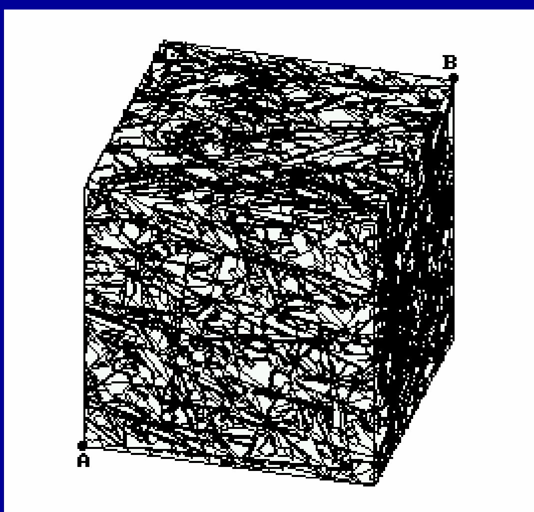

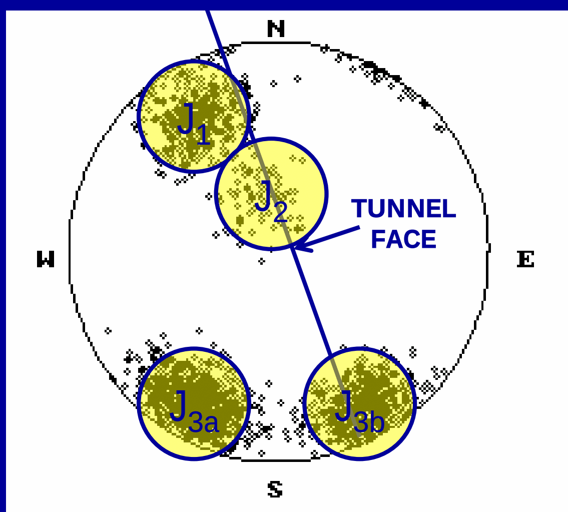

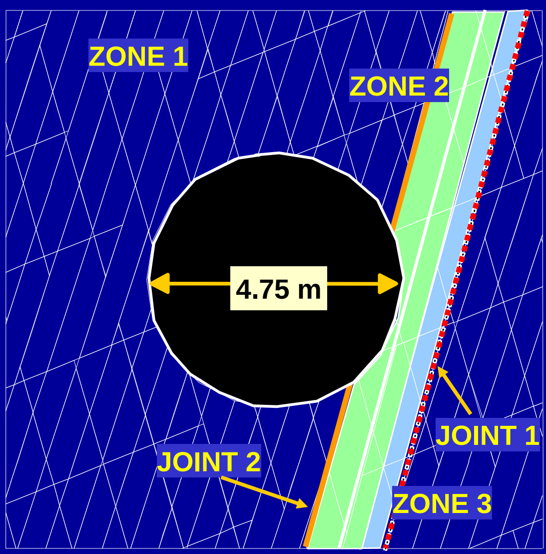

Detail of deterministic model

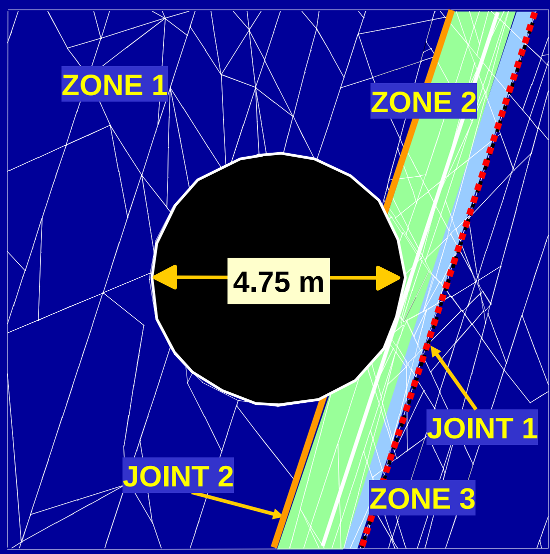

Detail of DFN model

PROPERTIES

Material Properties		Zone 1	Zone 2	Zone 3
E_m	[GPa]	60	30	10
ν_m	[-]	0.25	0.35	0.35
c	[MPa]	34	6.0	2.8
ϕ	[°]	38	36	34

Joint Properties		Zone 1	Zone 2	Zone 3	Joint 1 - 2
K_n	[GPa/m]	40	$5\ 10^{-3}$	$10\ 10^{-3}$	$1.25\ 10^{-3}$
K_s	[GPa/m]	4	$5\ 10^{-4}$	$10\ 10^{-4}$	$1.25\ 10^{-4}$
c	[MPa]	0.1	0	0	0
ϕ	[°]	33	22	22	22

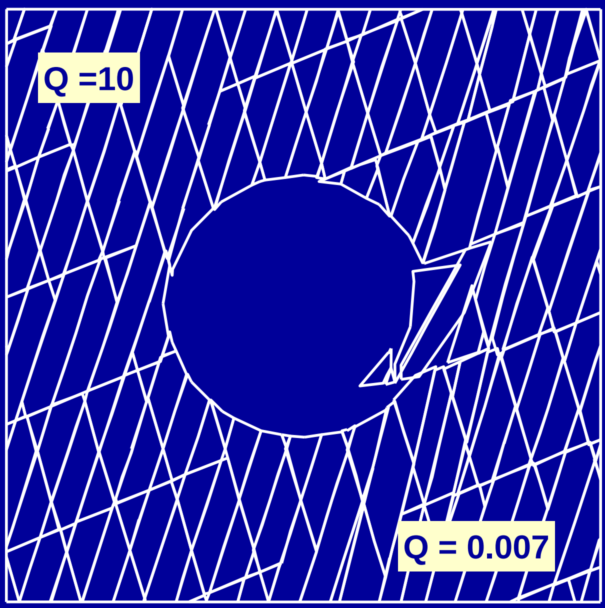

Detail of deterministic model

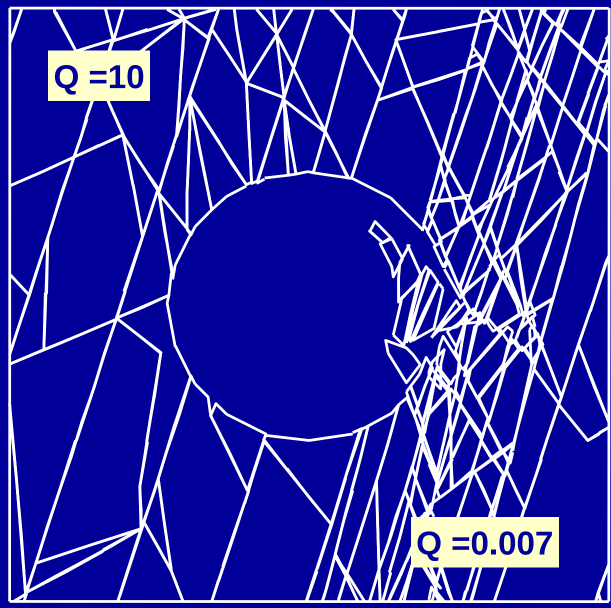

Detail of DFN model

BLOCK MOVEMENTS AROUND THE TUNNEL

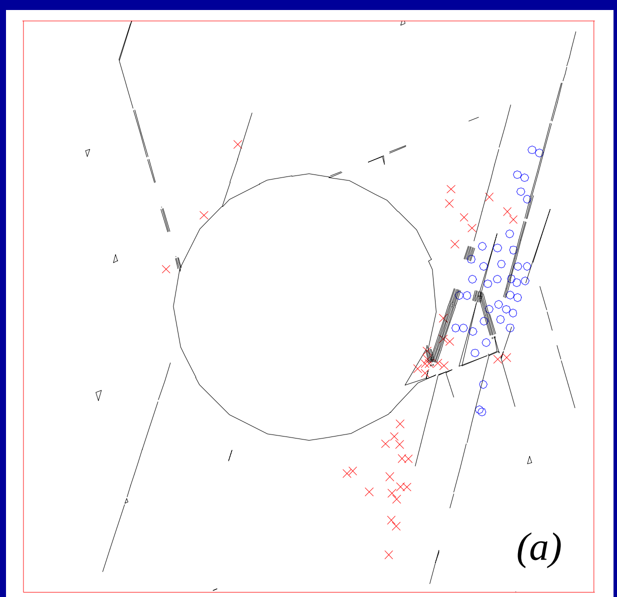

Detail of deterministic model

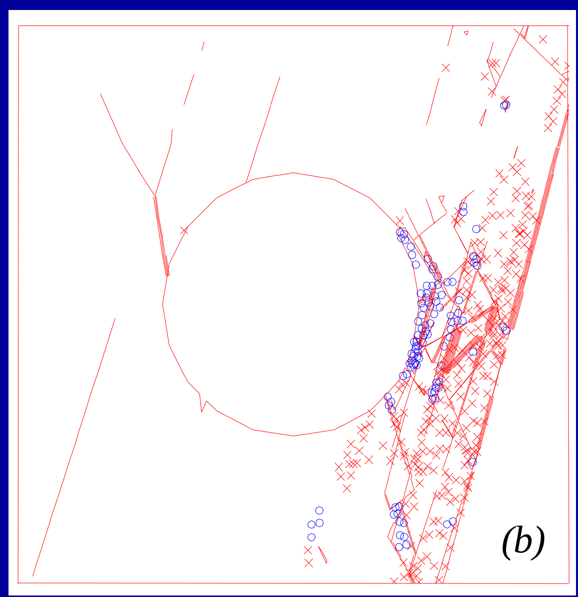

Detail of DFN model

YIELDED BLOCKS AND SHEAR DISPLACEMENTS AROUND THE TUNNEL

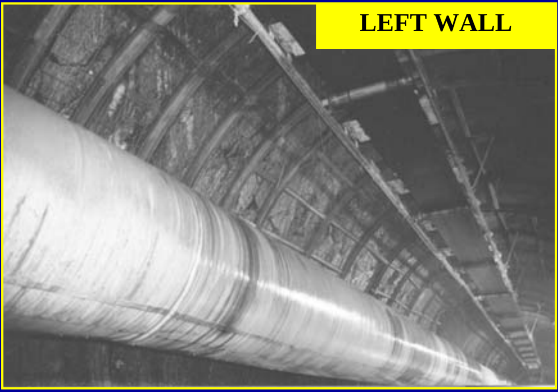

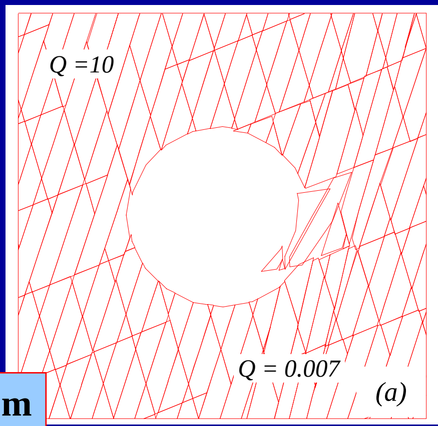

CH 2359 m

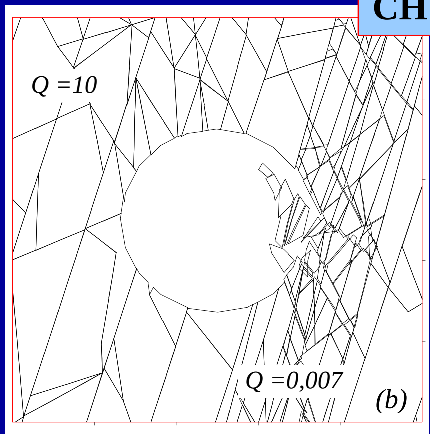

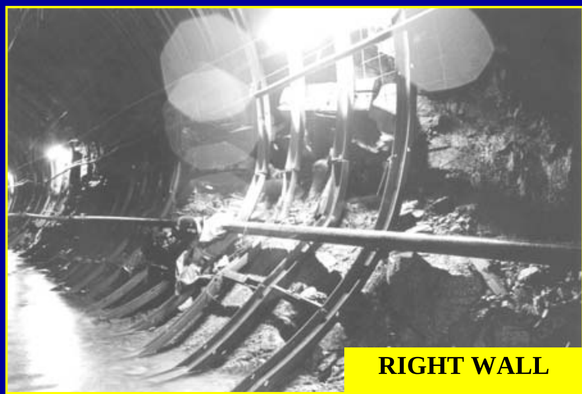

CHAINAGE 2742 m

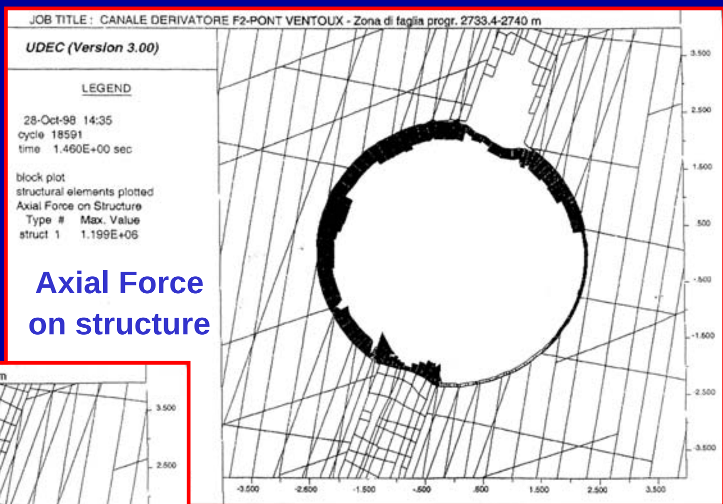

Axial Force on structure

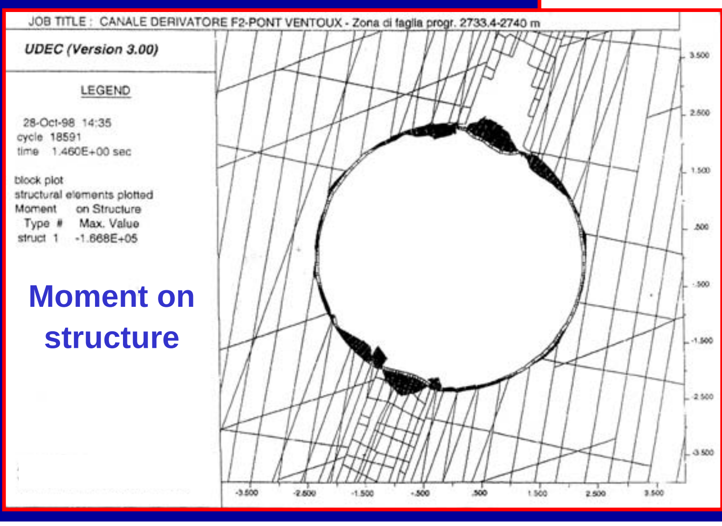

Moment on structure

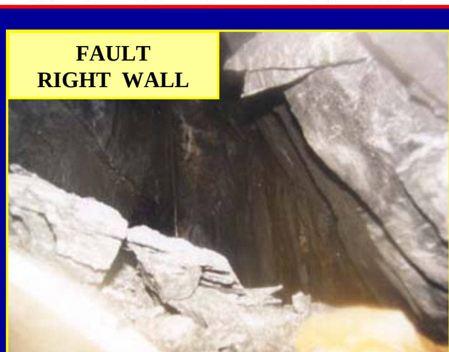

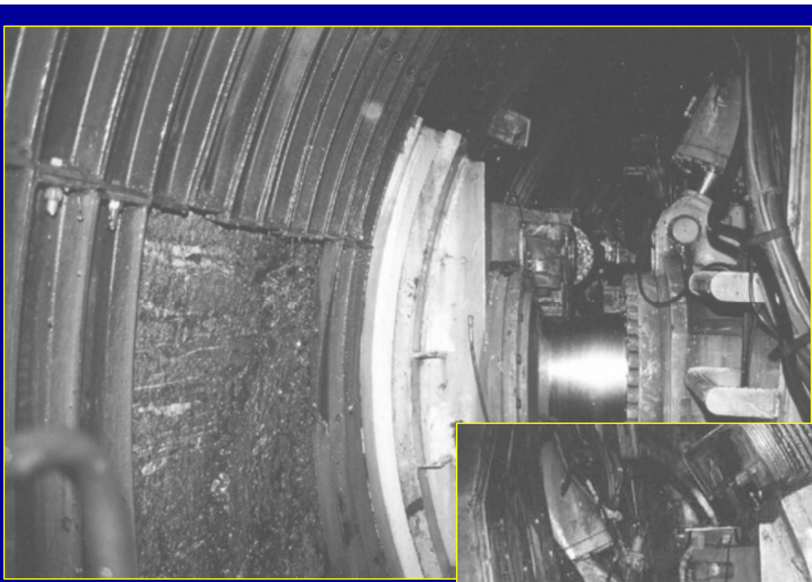

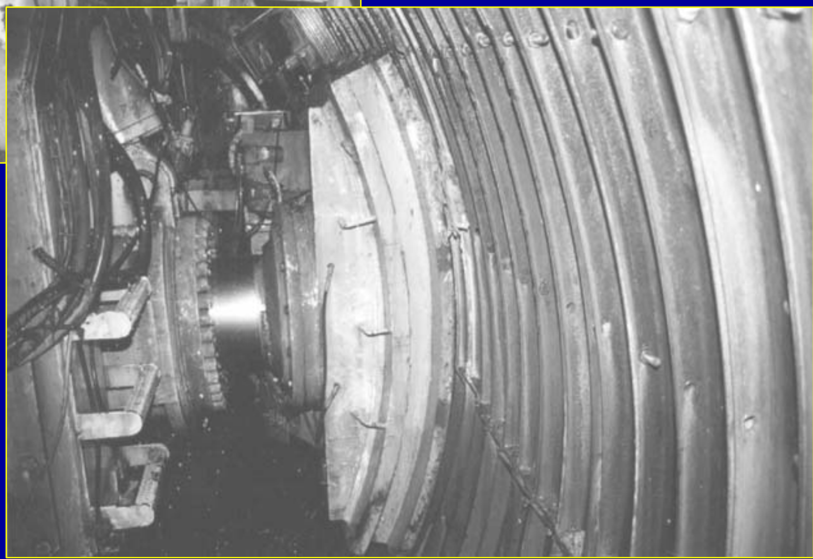

Conditions becoming difficult to require continuous placement of liner plates

Tunnels
Underground Excavations

Design Analyses
Case Studies and Observed Performance

Giovanni Barla

Department of Structural and Geotechnical Engineering